VISIT…

HYDRODYNAMIC LUBRICATION

H. J. Sneck and J. H. Vohr

FLUID FILM LUBRICATION

"Lubrication theory" begins with the Navier-Stokes equations and the continuity equation. Employing simplifications consistent with hydrodynamic lubrication, the end result is a set of relatively simple working equations which describe the velocity and pressure distribution throughout the flow field.

Assumptions which are made in lubrication theory are as follows. (1) the fluid film is very thin compared to its extent, (2) effects of gravity are negligible, (3) viscosity does not vary across the fluid film thickness, (4) curvature of the surfaces in journal bearings is large compared to the fluid film thickness, (5) the fluid adheres to solid boundaries with no slip, and (6) fluid inertia is negligible.

Reynolds Equation

The following equation which governs the pressure distribution within the fluid film is named after Osborne Reynolds who first derived it. Using the notation of Figure 1:

$$\frac{\partial}{\partial x}\left(\frac{\rho h^3}{\mu}\frac{\partial P}{\partial x}\right)+\frac{\partial}{\partial y}\left(\frac{\rho h^3}{\mu}\frac{\partial P}{\partial y}\right)=6\left\{\frac{\partial}{\partial y}\left[\rho(V_1+V_2)h\right]+\frac{\partial}{\partial x}\left[\rho(U_1+U_2)h\right]+2\rho\,(w_h-w_o)+2\frac{\partial(\rho h)}{\partial t}\right\} \quad (1)$$

Several simplifications can be made. It is usually possible to arrange the coordinate system so that $V_1 = V_2 = 0$, thereby eliminating the first right side term. Further, writing $U_1 + U_2 = U$ and taking x to be in the direction of U_1 and U_2 yields

$$\frac{\partial}{\partial x}\left(\frac{\rho h^3}{\mu}\frac{\partial P}{\partial x}\right)+\frac{\partial}{\partial y}\left(\frac{\rho h^3}{\mu}\frac{\partial P}{\partial y}\right)=6\left\{U\frac{\partial(\rho h)}{\partial x}+2\rho\,(w_h-w_o)+2\frac{\partial(\rho h)}{\partial t}\right\} \quad (2)$$

The first term on the right side of this equation indicates how the bearing surface motion combines with density gradients and the wedge action of the fluid film thickness to generate the pressure field. If the bearing walls are permeable, the net flow of fluid ($w_h - w_o$) through the porous walls contributes to the generation of pressure by the second right side term. The last term on the right side is the squeeze film term which relates density and film thickness variation with time and the fluid film pressure.

Usually the complete Reynolds equation is not needed for a specific problem. For incompressible fluids in bearings with impermeable walls ($w_h = w_o = 0$), for instance, density drops out and then

$$\frac{\partial}{\partial x}\left(\frac{h^3}{\mu}\frac{\partial P}{\partial x}\right)+\frac{\partial}{\partial y}\left(\frac{h^3}{\mu}\frac{\partial P}{\partial y}\right)=6U\frac{\partial h}{\partial x}+12\frac{\partial h}{\partial t} \quad (3)$$

A list of further simplifying conditions and the terms affected is provided in Table 1.

Infinite Slider Bearing

A better understanding of fluid film lubrication can be gained from a few simple bearing configurations. The infinitely long slider bearing shown in Figure 2 is one of these. The

Copyright © 1983 CRC Press LLC

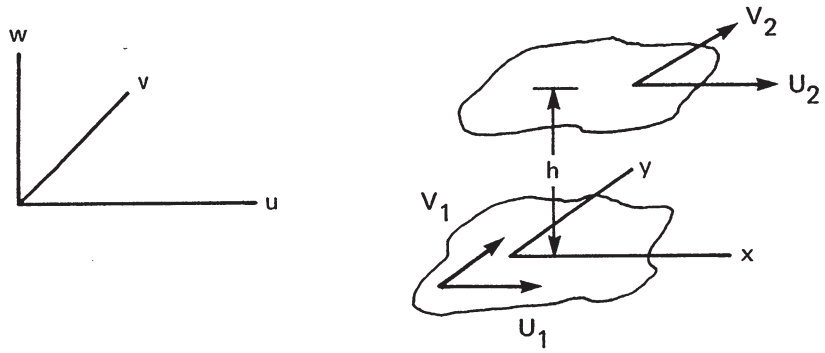

FIGURE 1. Coordinate direction and velocity components.

Table 1
SIMPLIFICATIONS TO THE GENERAL REYNOLDS EQUATION

Simplifying condition	Term simplified
1. Gas-lubricated bearing	Density ρ replaced by pressure P
2. Incompressible lubricant	Density ρ removed from equation
3. Bearing walls impermeable	$w_n = w_o = 0$
4. Film thickness does not vary with time	$\frac{\partial h}{\partial t} = 0$
5. Film thickness does not vary with x or y	$\frac{\partial h}{\partial x} = 0$
	$\frac{\partial}{\partial x}\left(\frac{\rho h^3}{\mu}\frac{\partial P}{\partial x}\right) = h^3\frac{\partial}{\partial x}\left(\frac{\rho}{\mu}\frac{\partial P}{\partial x}\right)$
	$\frac{\partial}{\partial y}\left(\frac{\rho h^3}{\mu}\frac{\partial P}{\partial y}\right) = h^3\frac{\partial}{\partial y}\left(\frac{\rho}{\mu}\frac{\partial P}{\partial y}\right)$
6. Viscosity does not vary with x or y	$\frac{\partial}{\partial x}\left(\frac{\rho h^3}{\mu}\frac{\partial P}{\partial x}\right) = \frac{1}{\mu}\frac{\partial}{\partial x}\left(\rho h^3\frac{\partial P}{\partial x}\right)$
	$\frac{\partial}{\partial y}\left(\frac{\rho h^3}{\mu}\frac{\partial P}{\partial y}\right) = \frac{1}{\mu}\frac{\partial}{\partial y}\left(\rho h^3\frac{\partial P}{\partial y}\right)$
7. Bearing surfaces do not move	$U\frac{\partial(\rho h)}{\partial x} = 0$
8. Bearing very long in y direction	$\frac{\partial}{\partial y}\left(\frac{\rho h^3}{\mu}\frac{\partial P}{\partial y}\right) \approx 0$
9. Bearing very short in y direction	$\frac{\partial}{\partial x}\left(\frac{\rho h^3}{\mu}\frac{\partial P}{\partial x}\right) \approx 0$

lower surface in Figure 2 moves to the left to draw the lubricant into a convergent wedge. Reynolds equation for a steady load with $\partial P/\partial y = 0$, an incompressible lubricant, and constant viscosity becomes

$$\frac{d}{dx}\left(h^3\frac{dP}{dx}\right) = -6U\mu\frac{dh}{dx} \qquad (4)$$

Copyright © 1983 CRC Press LLC

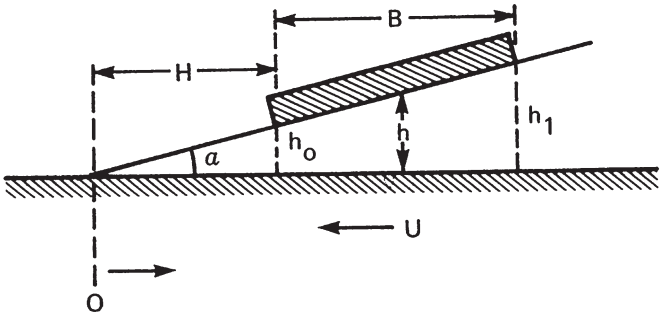

FIGURE 2. Slider bearings.

Table 2
INFINITE SLIDER BEARING PERFORMANCE

Quantity	Formula
Film thickness parameter	$K = \frac{h_1}{h_o} - 1$
Load capacity	$W = \frac{6U\mu B^2 L}{h_o^2 K^2} \left\{ \ln (1 + K) = \left(\frac{2K}{2 + K} \right) \right\}$
Friction force	$F_f = \frac{W}{2} \tan \alpha + \left(\frac{\mu UBL}{h_o K} \right) \ln (1 + K)$
Center of pressure	$\bar{X} = B \left\{ \frac{2(3 + K)(1 + K) \ln (1 + K) - K(6 + 5K)}{2K[(2 + K) \ln (1 + K) - 2K]} \right\}$

The film thickness shape is given by $(h_o/H)x$ where $H = h_o B/(h_1 - h_o)$. The first integral of this ordinary differential equation is

$$\frac{dP}{dx} = -6\, U\mu \left(\frac{h - \bar{h}}{h^3} \right) \tag{5}$$

Constant of integration $\bar{h}$ is also the film thickness at which the pressure is a maximum and where dP/dx = 0. If the film thickness did not converge, h would be constant throughout the film and no pressure buildup could occur. Integrating a second time yields

$$P = -\frac{6U\mu B}{h_1 - h_o} \left(\frac{\bar{h}}{2h^2} - \frac{1}{h} + c \right) \tag{6}$$

Using the boundary conditions of P = 0 at h = 0 and h = h_1 to evaluate integratior constants $\bar{h}$ and c, the pressure in the slider becomes

$$P = \frac{6U\mu B}{h_1 - h_o} \left[\frac{1}{h} - \frac{h_o h_1}{h^2 (h_1 + h_o)} - \frac{1}{h_o + h_1} \right] \tag{7}$$

The pressure and the load it supports are directly proportional to surface velocity U and viscosity μ. Table 2 summarizes the performance characteristics of an infinitely wide slider bearing.

Copyright © 1983 CRC Press LLC

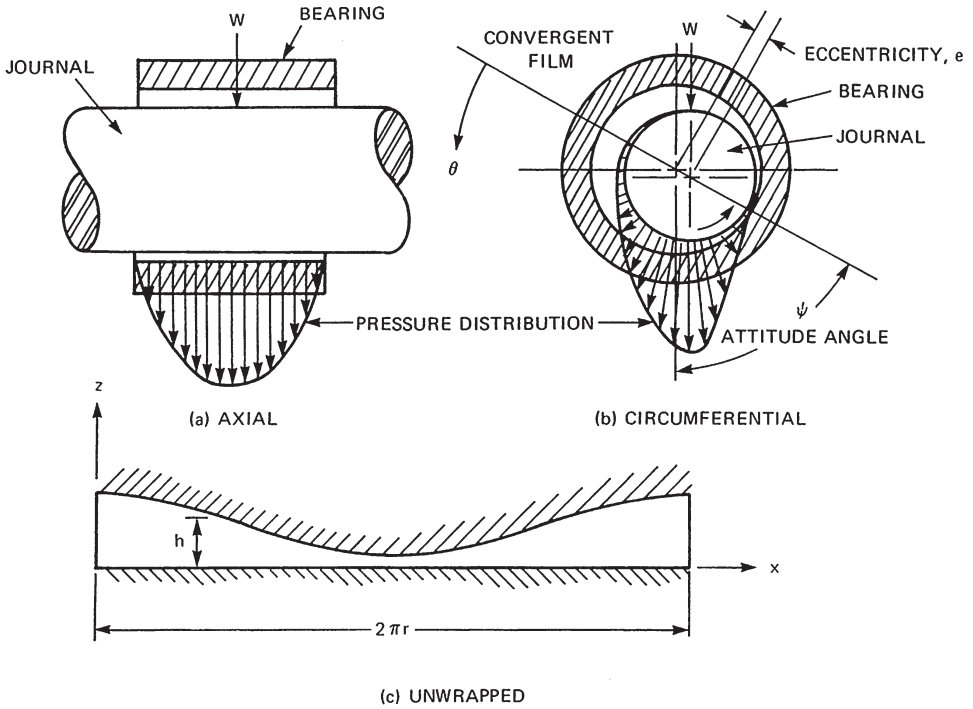

FIGURE 3. Journal bearing oil-film relations.

Short Journal Bearing

The three factors essential for a hydrodynamic slider bearing (velocity, viscosity, and a converging film) are all contained in the right side term of the Reynolds equation 6 μU(dh/dx). The required convergent film is also formed when a shaft and bushing become eccentric as shown in Figure 3b.

The unwrapped film shape is shown in Figure 3c. A positive superambient pressure is generated in the convergent left portion of the film. Since liquids cannot withstand substantial subambient pressure, the fluid film ruptures in the divergent right section, forming discontinuous streamers which flow through this region at approximately ambient pressure. These streamers contribute nothing to load carrying capacity.

When the bearing is "narrow", i.e., its length is less than its diameter, Reynolds equation can be simplified to

$$h^3 \frac{\partial^2 P}{\partial y^2} = 6\,U\mu \frac{dh}{dx} \tag{8}$$

Neglecting the pressure gradient term for the x direction attributes circumferential flow primarily to the motion of the journal surface expressed by the right side of the equation. Axial flow and leakage are due entirely to the pressure gradient term on the left side of the equation.

This "short bearing" version of Reynolds equation can be integrated twice in the y direction, because h is not a function of y, to give the pressure function

$$P = \frac{3U\mu}{h^3} \frac{dh}{dx} \left[y^2 - \left(\frac{L}{2} \right)^2 \right] \tag{9}$$

Copyright © 1983 CRC Press LLC

Table 3
SHORT JOURNAL BEARING

Quantity	Formula
Load capacity	$W = \frac{U\mu L^3 \pi}{4c^2} \left[\frac{\epsilon}{(1-\epsilon^2)^2}\right] (0.62\,\epsilon^2 + 1)^{1/2}$
Attitude angle	$\tan\psi = \frac{\pi}{4} \frac{(1-\epsilon^2)^{1/2}}{\epsilon}$
Friction force	$F_f = \frac{c\epsilon W \sin\psi}{2r} + \frac{2\pi\mu UrL}{c(1-\epsilon^2)^{1/2}}$
Oil flow from ends of bearing	$Q = UcL\epsilon$

where y is measured from the bearing center plane. This distribution satisfies the pressure boundary conditions of P = 0 at both y = L/2 and y = –L/2.

Axial pressure distribution is shown by this equation to approach a simple parabolic shape. Because the fluid film thickness is much smaller than the journal radius, $h = c(1 - \epsilon\cos\theta)$. When substituted into the pressure equation

$$P = \frac{3\,U\mu\epsilon\sin\theta}{rc^2(1+\epsilon\cos\theta)^3}\left[\left(\frac{L}{2}\right)^2 - y^2\right] \tag{10}$$

Positive pressures are obtained in the convergent wedge portion between 0 and π. A reasonably accurate prediction of load capacity can be obtained by setting the pressure equal to zero in the divergent region between π and 2 π.

Retaining the axial pressure gradient term which accounts for axial flow allows a more realistic treatment of axial pressure distribution than with the infinite slider bearing approximation. Table 3 summarizes the performance characteristics of a short journal bearing. A comprehensive table of integrals is available for use in solution of the sin-cos relations commonly encountered with journal bearings.[1]

When the shaft is lightly loaded, the eccentricity ratio, ϵ, approaches zero, The following Petroff equation results from Table 3 and is frequently used to estimate journal bearing power loss.

$$F_f = 2\pi\,\mu\,U\,rL/c \tag{11}$$

Cylindrical Coordinates

Reynolds equation in cylindrical coordinates (used in analysis of circular thrust bearings) is

$$\frac{1}{r}\frac{\partial}{\partial r}\left(\frac{\rho r h^3}{\mu}\frac{\partial P}{\partial r}\right) + \frac{1}{r^2}\frac{\partial}{\partial\phi}\left(\frac{\rho h^3}{\mu}\frac{\partial P}{\partial\phi}\right) = \frac{6\mu}{r}\left[\frac{\partial}{\partial r}(\rho h r\,U_r) + \frac{\partial}{\partial\phi}(\rho h\,V_\phi) + 2\rho\,(w_h - w_o)\,r\right] \tag{12}$$

where U_r and V_ϕ, the radical and tangential surface velocities, play the same roles as U and V in rectangular coordinates.

TURBULENCE

Very high speeds, large clearances, or low-viscosity lubricants may introduce a sufficiently

Copyright © 1983 CRC Press LLC

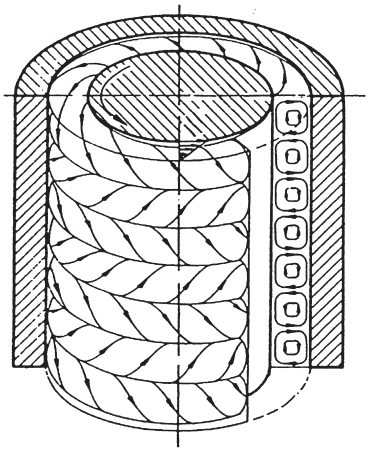

FIGURE 4. Taylor vortices between concentric rotating cylinders with the inner cylinder rotating. (From Schlichting, H., *Boundary Layer Theory,* 6th ed., McGraw-Hill, New York. 1968. With permission.)

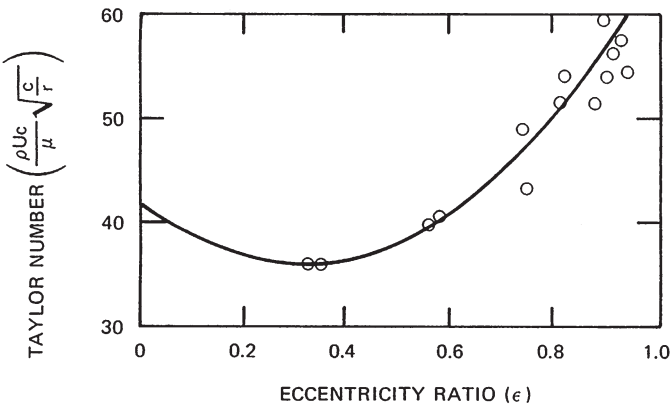

FIGURE 5. Critical Taylor number vs. eccentricity ratio. Experimental results for c/r = 0.00494. (From Frene J. and Godet, M., *Trans. ASME Ser. F,* 96, 127, 1974. With permission.)

high Reynolds number in a bearing film for departure from laminar flow velocity by either of two instabilities: Taylor vortices or turbulence.

Taylor vortex flow is characterized by ordered pairs of vortices between a rotating inner cylinder and an outer cylinder as shown in Figure 4.[2] Such vortices significantly "flatten" the velocity profile between the cylinders and increase the wall shear stress. For a concentric cylindrical journal bearing, vortices develop when the Taylor number $\rho Uc\sqrt{c/r}/\mu$ exceeds 41.1.[3] For nonconcentric (loaded) bearings the situation is less clear, although studies have recently been made.[4-8] Critical Taylor numbers are shown in Figure 5 as a function of eccentricity.[7]

Turbulence is a more familiar phenomenon. Unlike Taylor vortices, disordered flow in turbulence is not produced by centrifugal forces and will occur whether the inner or outer cylinder is rotating. In experimental studies where turbulence develops before Taylor vortices,[9] turbulence appears to set in when the Reynolds number $Re = \rho Uc/\mu$ exceeds 2000.

Copyright © 1983 CRC Press LLC

When vortices develop first, turbulence may begin at a lower value of Reynolds number.[4] Assuming that vortices develop when Re $\sqrt{c/r}$ = 41.1, vortices will occur before turbulence for c/r ratios greater than 0.0004. In most bearings, however, turbulence sets in shortly after the development of vortices; and since random turbulent momentum transfer appears to dominate, turbulent lubrication theories have neglected the effect of vortices.

Turbulent lubricating film theories have been based on well-established empiricisms such as Prandtl mixing length or eddy diffusivity.[10-12] Most commonly employed is that due to Elrod and Ng[11] based on eddy diffusivity. Volume flows in the film are related to pressure gradient through turbulent lubrication factors G_x and G_y, i.e.

$$\overline{uh} = q_x = -G_x (h^3/\mu)\, \partial P/\partial x + r\omega h/2 \tag{13}$$

$$\overline{vh} = q_y = -G_y (h^3/\mu)\, \partial P/\partial y \tag{14}$$

where x refers to the circumferential direction and y axial. Flows $\overline{uh}$ and $\overline{vh}$ are obtained from integrating velocities u and v across the film thickness. G_x and G_y depend upon the level of turbulence as a function of local Reynolds number $\overline{U}h/\nu$ where $\overline{U}$ is the local mean fluid film velocity. For Couette flow $Re_c = Uh/\nu$, where U is the bearing surface velocity, while for pressure induced flow $Re_p = |\nabla P|h^3/\mu\nu$ where $|\nabla P|$ denotes the absolute magnitude of the pressure gradient.

Using Equations 13 and 14 for lubricant flow rates, the turbulent Reynolds equation is obtained:

$$\frac{\partial}{\partial x}\left(\frac{G_x}{\mu} h^3 \frac{\partial P}{\partial x}\right) + \frac{\partial}{\partial y}\left(\frac{G_y}{\mu} h^3 \frac{\partial P}{\partial y}\right) = \frac{U}{2}\frac{\partial h}{\partial x} \tag{15}$$

While G_x and G_y depend, in general, upon the pressure gradient, they become functions of Re_c alone at very high surface velocities and high Re_c In Figure 6, considering the curve corresponding to $Re_p = 10^6$, G_x at $Re_c = 2 \times 10^4$ joins an envelope of curves and becomes independent of Re_p provided Re_p remains less than 10_6 and Re_c remains greater than 10^4.

For most hydrodynamic bearings, "linearized theory" with values of G_x given by the limiting envelope in Figure 6 suffices to describe turbulence.[13] Appropriate values of G_x and G_y are given by the following.[14]

$$1/G_x = 12 + 0.0136\,(Re_c)^{0.90}$$

$$1/G_y = 12 + 0.0043\,(Re_c)^{0.96} \tag{16}$$

While various "fairing" procedures have been applied in the uncertain transition region between laminar and turbulent flow,[15] the writer favors the following procedure. For values of Re_c less than 41.2 $\sqrt{r/c}$ (onset of vortices), laminar flow theory is to be used. For values of Re_c greater than 2000, fully developed turbulent relationships such as Equation 16 are to be used. Between these critical values of Re_c, linearly interpolate between the laminar values for G_x and G_y (i.e., 1/12) and the values for G_x and G_y evaluated at Re_c = 2000, with Re_c being the interpolation variable.

A critical parameter affected by turbulence is the shear stress τ_s acting on the sliding member of a hydrodynamic bearing. For motion in the x direction, τ_s under laminar flow conditions is

$$\tau_s = \tau_c + h/2\,\frac{\partial P}{\partial x} \tag{17}$$

Copyright © 1983 CRC Press LLC

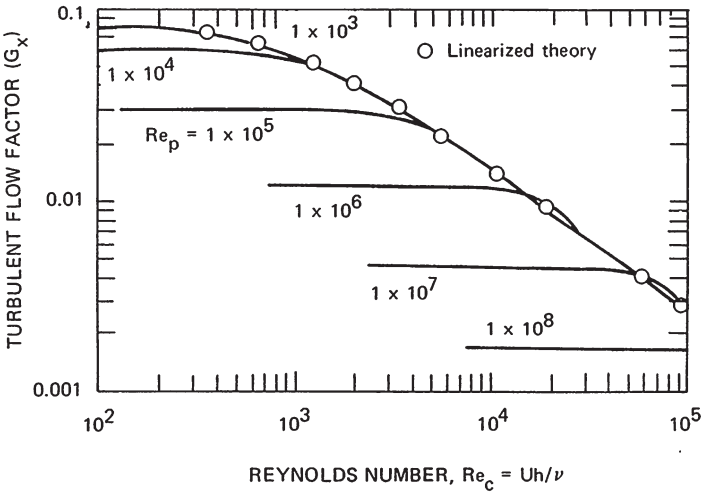

FIGURE 6. Turbulent flow factor G_x for $\partial p/\partial x$ negative and $\partial p/\partial y = 0$.

where Couette shear stress $\tau_c = \mu U/h$. Onset of turbulence increases both τ_c and $\partial P/\partial x$. The increase in $\partial P/\partial x$ is calculated through the turbulent Reynolds Equation 15. The increase in τ_c is taken account of through turbulent Couette shear stress factor C_f, i.e.,

$$\tau_c = C_f \mu U/h \tag{18}$$

Values of C_f are reasonably approximated from linearized theory by the following:[13,14]

$$C_f = 1 + 0.0012 (Re_c)^{0.94} \tag{19}$$

Qualitatively, turbulence increases apparent viscosity of the film and hence increases load capacity and power loss above that with laminar flow. If C_f is calculated to be say, 1.25, the concentric turbulent power loss would be 25% higher than that predicted for laminar flow. Enhancement of load capacity is illustrated in Figure 7.

For turbulence in externally pressurized bearings, e.g. for cryogenic turbopumps[16] dominated by pressure-induced flow, turbulent flow factors G_x and G_y become functions only of Re_p, as shown in Figure 8. An iterative procedure is usually needed to solve for the pressure gradient. Convergence is usually rapid.

Relatively little attention has been given to transition to turbulence in thrust bearings. Pad temperatures of tilting pad bearings reported by Capitao, Gregory, and Whitford[17] show a sharp decrease as operating speed is increased beyond a certain critical value, dependent upon load. This temperature decrease is due apparently to onset of turbulence, which drastically increases heat transfer from the pads to the oil in the grooves between pads.[18] Calculations of local Reynolds numbers by Roben[19] show "transition" Reynolds numbers in the range 1000 to 1200. This is somewhat higher than the range 580 to 800 suggested by Abromovitz[20] and supported by Gregory.[21] The discrepancy may reflect that the lower range cited pertains to an average Reynolds number for the bearing pad.

Since the turbulent lubrication theories discussed above neglect centrifugal vortex effects, they apply to thrust bearings as well as to journal bearings.

Copyright © 1983 CRC Press LLC

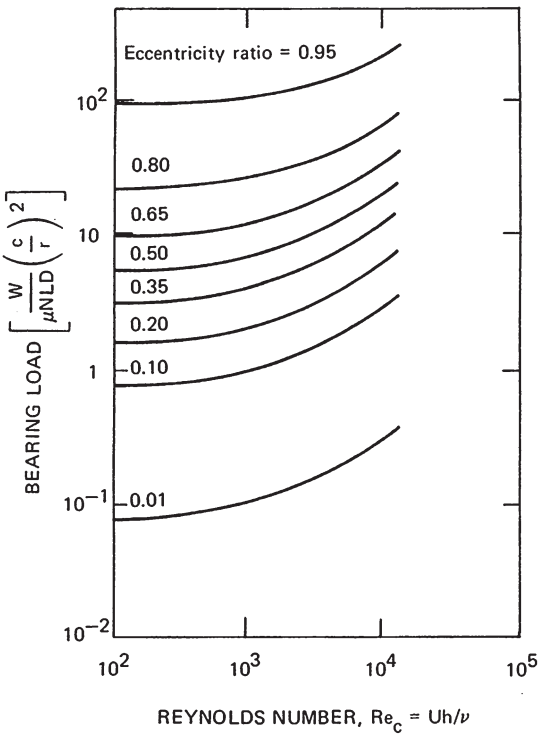

FIGURE 7. Load capacity of turbulent full journal bearing for L/D = 1. (From Ng. C. W. and Pan, C. H. T., *Trans. ASME,* 87(4), 675. 1965. With permission.)

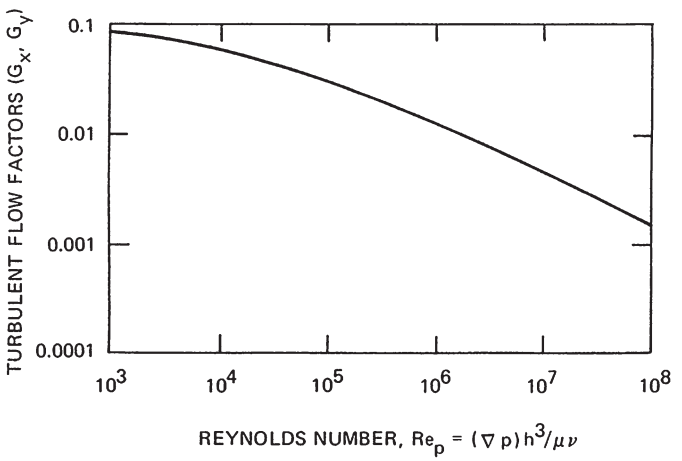

FIGURE 8. Turbulent velocity parameters G_x and G_y vs. Re_p when turbulence is dominated by pressure-induced flow. (From Reddeclif, J. M. and Vohr, J. H., *J. Luhr. Technol. Trans. ASME Ser. F,* 91(3), 557, 1969. With permission.)

ENERGY EQUATION

Temperature distribution in the lubricant film is governed by the energy equation which may be derived from the differential element of bearing film shown in Figure 9. The top bounding surface is assumed stationary while the bottom surface moves with velocity U in

Copyright © 1983 CRC Press LLC

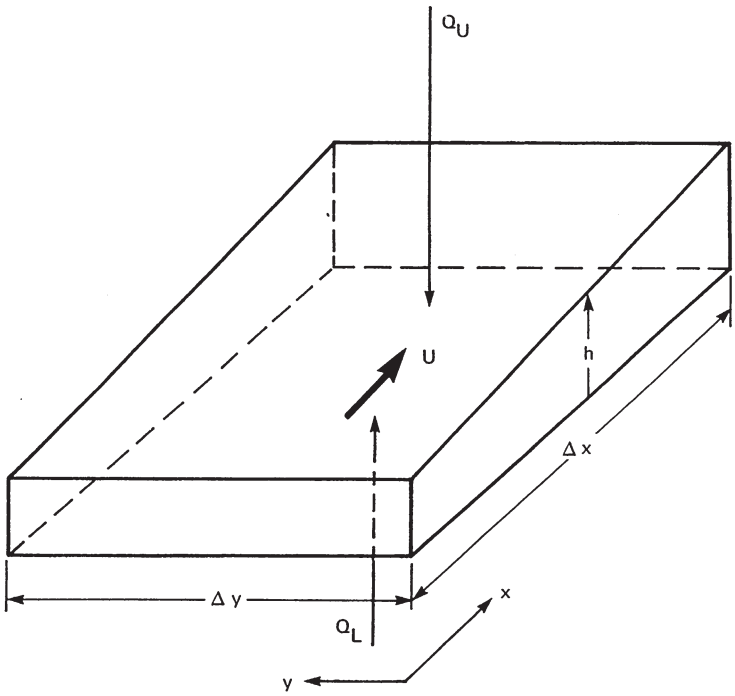

FIGURE 9. Control volume for energy conservation.

the x direction. Considering steady flow and neglecting (1) variations in fluid properties, (2) kinetic and potential energy of the fluid, and (3) variations in temperature normal to the x-y plane, energy convected into the differential volume is given by

$$E_{in} = \rho c_p q_x (x,y + \Delta y/2)\ T(x,y + \Delta y/2)\ \Delta y + \rho c_p q_y (x + \Delta x/2, y)\ T (x + \Delta x/2,y)\ \Delta x \quad (20)$$

while the energy convected out by the flow of lubricant is

$$E_{out} = \rho c_p q_x (x + \Delta x, y + \Delta y/2)\ T (x + \Delta x,y + \Delta y/2)\ \Delta y + \rho c_p q_y (x + \Delta x/2,y + \Delta y)\ T (x + \Delta x/2,y + \Delta y)\ \Delta x \quad (21)$$

where q_x and q_y are the volume fluxes of lubricant in $m^3/m/sec$ in the x and y directions, respectively.

Conduction of heat in the x and y directions is neglected as compared with convection. Heat conducted *into* the control volume in the z direction may be expressed simply as $Q_U \Delta x \Delta y$ and $Q_L \Delta x \Delta y$ where Q_U and Q_L represent conduction heat fluxes through the upper and lower bearing surfaces in W/m^2.

Pressure work done on the lubricant entering and by the lubricant leaving is as follows:

$$W_{in} = P(x,y + \Delta y/2)\ q_x (x,y + \Delta y/2)\ \Delta y + P(x + \Delta x/2,y)\ q_y (x + \Delta x/2,y)\ \Delta x$$

$$W_{out} = P(x + \Delta x,y + \Delta y/2)\ q_x (x + \Delta x,y + \Delta y/2)\Delta y + P(x + \Delta x/2,y + \Delta y)\ q_y (x + \Delta x/2,y + \Delta y)\ \Delta x \quad (22)$$

Copyright © 1983 CRC Press LLC

Work done on the lubricant by shear stress τ_s at the moving surface is given by $\tau_s U \Delta x \Delta y$. Equating net heat flow convected and conducted out of the control volume to work done on the fluid, dividing through by Δx and Δy, taking the limit as Δx and Δy go to zero, and applying the following continuity equation

$$\partial q_x/\partial x + \partial q_y/\partial y = 0 \tag{23}$$

results in the following overall energy balance

$$\rho c_p \left[q_x \frac{\partial T}{\partial x} + q_y \frac{\partial T}{\partial y} \right] = Q_u + Q_L - q_x \frac{\partial P}{\partial x} - q_y \frac{\partial P}{\partial y} + \tau_s U \tag{24}$$

For laminar flow, the lubricant fluxes q_x and q_y are given by:

$$q_x = \frac{-h^3}{12\mu} \frac{\partial P}{\partial x} + \frac{Uh}{2}$$

$$q_y = \frac{-h^3}{12\mu} \frac{\partial P}{\partial y} \tag{25}$$

These expressions may be modified to take account of turbulence by means of the turbulent flow factors G_x and G_y described earlier.

$$q_x = \frac{-G_x h^3}{\mu} \frac{\partial P}{\partial x} + \frac{Uh}{2}$$

$$q_y = \frac{-G_y h^3}{\mu} \frac{\partial P}{\partial y} \tag{26}$$

Stress τ_s at the moving surface is given for laminar flow by the first of the following relations, and is modified in the second case by turbulence factor C_f discussed earlier.

$$\tau_s = \frac{\mu U}{h} + \frac{h}{2} \frac{\partial P}{\partial x}$$

$$\tau_s = C_f \mu \frac{U}{h} + \frac{h}{2} \frac{\partial P}{\partial x} \tag{27}$$

Since Equation 24 depends upon the pressure gradient, it must be solved simultaneously with the Reynolds equation. The usual procedure assumes an initially uniform temperature (and viscosity) distribution to solve Reynolds equation for P(x,y); q_x, q_y, and τ_s are then determined from Equations 26 and 27. Equation 24 is then solved for T(x,y) and hence μ(T). Reynolds equation is then resolved for pressure using the new distribution for viscosity. This iterative procedure typically converges quickly.

Equation 24 requires specification of a bearing film inlet temperature. This temperature is usually higher than that of the oil supplied to the bearing as a result of (1) heating as the oil comes into contact with bearing metal parts, and (2) hot oil recirculation in and around the bearing.

DYNAMICS

Three important concerns are commonly associated with the dynamic behavior of bearings: (1) avoiding any bearing-rotor system natural frequencies, or "critical speeds", near op-

Copyright © 1983 CRC Press LLC

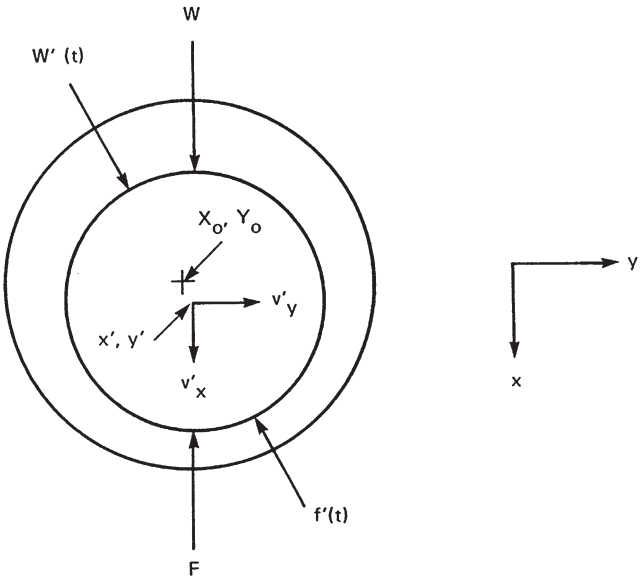

FIGURE 10. Dynamic motion of shaft.

erating speeds, (2) limiting forced vibrations of the rotor-bearing system to acceptable levels, and (3) freedom from self-excited "half frequency whirl" or "oil whip" instability.

Dynamic motion of a shaft in a fluid film bearing is illustrated in Figure 10. In general, steady load W is balanced by steady film force F. Superposed dynamic loading $W'(t)$ produces dynamic shaft displacement $x'(t)$ and $y'(t)$ away from steady state position x_o, y_o, Corresponding dynamic bearing film forces $f_x'(t)$ and $f_y'(t)$ may be calculated from Reynolds equation since film thickness h and the time rate of change of h can be determined if x', y', and v'_x, and v'_y are known.

From instantaneous film forces $f_x'(0$ and $f_y'(t)$, dynamic motions of a rigid shaft of mass M can be determined from the following equations of motion:

$$M \frac{d^2x'}{dt^2} = f_x'(t) + W_x'(t)$$

$$M \frac{d^2y'}{dt^2} = f_y'(t) + W_y'(t) \qquad (28)$$

where $W_x'(t)$ and $W_y'(t)$ represent the x and y components of the externally imposed dynamic loading on the shaft.

Since $f_x'(t)$ and $f_y'(t)$ are, in general, determined by a numerical solution of Reynolds equations, Equations 28 may be solved numerically by a time integration procedure. This "nonlinear transient analysis" does not involve the common simplifying assumption that a linear relationship exists between shaft motions and the bearing film forces f_x' and f_y'. This transient approach is usually cumbersome and expensive since Reynolds equation must be solved at each time step, and many cycles of shaft motion may need to be analyzed to define rotor-bearing critical speeds, response to forced vibrations, and rotor bearing stability.

When using linearized stiffness and damping coefficients, shaft motions are assumed to be sufficiently small that dynamic bearing forces f_x' and f_y' are linearly proportional to journal displacements x' and y' and to journal velocities v_x' and v_y'.

$$-f_x' = K_{xx}x' + K_{xy}y' + B_{xx}v_x' + B_{xy}v_y' \qquad (29)$$

Copyright © 1983 CRC Press LLC

$$-f_{y'} = K_{yx}x' + K_{yy}y' + B_{yx}v_{x}' + B_{yy}v_{y}' \tag{30}$$

Proportionality constants K_{xx}, K_{xy}, K_{yx}, and K_{yy} are referred to as bearing spring coefficients while B_{xx}, B_{xy}, B_{yx}, and B_{yy} are bearing damping coefficients.

The usual computational procedure for determining the stiffness coefficients is to solve Reynolds equation for bearing force components $F_x(x_o y_o)$ and $F_y(x_o y_o)$ with the journal steady-state position x_o,y_o. For a very small shift, δ, of the journal in the x direction, bearing forces $F_x(x_o + \delta, y_o)$ and $F_y(x_o + \delta, y_o)$ are then recalculated. Stiffness coefficients K_{xx} and K_{yx} are given approximately by:

$$K_{xx} = \frac{F_x(x_o + \delta, y_o) - F_x(x_o, y_o)}{\delta}$$

$$K_{yx} = \frac{F_y(x_o + \delta, y_o) - F_y(x_o, y_o)}{\delta} \tag{31}$$

K_{xy} and K_{yy} are similarly computed from a small journal displacement in the y direction.

Damping coefficients B_{xx}, B_{xy}, etc. are calculated by solving Reynolds equation to determine the bearing squeeze film forces that arise due to journal velocities v_x' and v_y'. For incompressible lubricants, squeeze film forces are linearly proportional to squeezing velocity provided boundary conditions for the pressure solution do not change.

Substituting Equations 29 and 30 into Equation 28 gives the equations of motion of a rigid rotor supported in a fluid film bearing. Velocities v_x' and v_y' in Equations 29 and 30 are replaced by their equivalents dx′/dt and dy′/dt.

$$M\frac{d^2x'}{dt^2} = W_{x'} - K_{xx}x' - K_{xy}y' - B_{xx}\frac{dx'}{dt} - B_{xy}\frac{dy'}{dt} \tag{32}$$

$$M\frac{d^2y'}{dt^2} = W_{y'} - K_{yx}x' - K_{yy}y' - B_{yx}\frac{dx'}{dt} - B_{yy}\frac{dy'}{dt} \tag{33}$$

Coupled linear Equations 32 and 33 relate bearing dynamic motions x′ and y′ to the imposed dynamic load components $W_x'(t)$ and $W_y'(t)$. Following four solutions of the associated Reynolds equations to determine the eight stiffness and damping coefficients, Equations 32 and 33 are then solved for "bearing response" and "bearing stability".

Bearing Natural Frequency

Natural frequencies of a rigid rotor are those at which the rotor would tend to vibrate if it were initially disturbed and then left free to return to steady state equilibrium. Natural frequencies of rotor-bearing systems are referred to as critical speeds because large vibration response is often experienced when running speed is the same as the natural frequency. Mathematically, these natural frequencies for a single bearing are determined by equations of motion 32 and 33 with dynamic forces $W'_x(t)$ and $W'_y(t)$ set equal to zero. The solution to this set of equations may be expressed in the form:

$$x'(t) = \text{Real}\{x^* e^{st}\}$$
$$y'(t) = \text{Real}\{y^* e^{st}\} \tag{34}$$

where x* and y* are complex amplitudes which are not functions of time and where $s = \lambda + i\nu$ is a complex "frequency". Acutal motion x′(t) is given by the real part of the complex number formed by multiplying x* and e^{st}. The last terms can be given as

$$e^{st} = e^{\lambda} e^{i\nu t} = e^{\lambda\tau}(\cos \nu t + i \sin \nu t) \tag{35}$$

Copyright © 1983 CRC Press LLC

If we denote $x^* = \alpha + i\beta$, then

$$x'(t) = e^{\lambda t}(\alpha \cos \nu t - \beta \sin \nu t) \tag{36}$$

Differentiating Equation 34 we find that

$$\frac{dx'}{dt} = \text{Real}\{s x^* e^{st}\}$$

$$\frac{d^2x'}{dt^2} = \text{Real}\{s^2 x^* e^{st}\} \tag{37}$$

Thus we obtain from Equations 32 and 33

$$\text{Real}\{[Ms^2 x^* + B_{xx}s x^* + B_{xy}s y^* + K_{xx}x^* + K_{xy}y^*] e^{st}\} = 0 \tag{38}$$

$$\text{Real}\{[Ms^2 y^* + B_{yx}s x^* + B_{yy}s y^* + K_{yx}x^* + K_{yy}y^*] e^{st}\} = 0 \tag{39}$$

With the real part of the complex number inside the brackets forced to be zero, canceling out the common term e^{st} gives the following simultaneous equations for x* and y* in matrix form.

$$\begin{bmatrix} Ms^2 + B_{xx}s + K_{xx} & B_{xy}s + K_{xy} \\ B_{yx}s + K_{yx} & Ms^2 + B_{yy}s + K_{yy} \end{bmatrix} \begin{Bmatrix} x^* \\ y^* \end{Bmatrix} = 0 \tag{40}$$

According to linear equation theory, nonzero solutions for natural vibration amplitudes x* and y* will be obtained if and only if the determinant of the left side matrix in Equation 40 is zero. This leads to the following characteristic equation for s:

$$Ms^4 + M(B_{xx} + B_{yy})s^3 + [M(K_{xx} + K_{yy}) + (B_{xx}B_{yy} - B_{yx}B_{xy})]s^2 + (B_{xx}K_{yy} + B_{yy}K_{xx} - B_{yx}K_{xy} - B_{xy}K_{yx})s + K_{xx}K_{yy} - K_{yx}K_{xy} = 0 \tag{41}$$

Many "canned" computer routines are available for ready solution of this fourth order polynomial equation for complex number s. Solutions for s occur in complex conjugate pairs, i.e., the four solutions for s are

$$s_1 = \lambda_1 + i\nu_1$$

$$s_2 = \lambda_1 - i\nu_1$$

$$s_3 = \lambda_2 + i\nu_2$$

$$s_4 = \lambda_2 - i\nu_2 \tag{42}$$

That is, dynamic vibration x′(t), in the absence of an external forcing function, will decay back to an equilibrium state at a rate given by the exponential decay factor λ_1 and λ_2, and at frequency ν_1 or ν_2. If the damping factor roots λ_1 and λ_2 are both negative, the bearing is stable: free vibrations will tend to die out. On the other hand, if either λ_1 or λ_2 is positive, then vibration will tend to grow without external excitation, an unstable condition.

For a simplified calculation of bearing natural frequencies, consider a bearing in which cross-coupling stiffness terms K_{xy} and K_{yx} are zero. Tilting pad bearings satisfy this condition.

Copyright © 1983 CRC Press LLC

As a further simplification, neglect damping in the solution for v_1 and v_2. This simplification is valid for bearings having negligible cross-coupling stiffness and damping coefficients, but is often not valid for fixed-arc bearings where the cross-coupling terms are significant.

With these simplifying assumptions, the bearing coefficient matrix becomes simply

$$\begin{bmatrix} K_{xx} + Ms^2 & \\ & K_{yy} + Ms^2 \end{bmatrix}$$

The characteristic equation for s is

$$(K_{xx} + Ms^2)\,(K_{yy} + Ms^2) = 0 \tag{43}$$

where solutions are

$$s_1 = i\sqrt{\frac{K_{xx}}{M}}$$

$$s_2 = -i\sqrt{\frac{K_{xx}}{M}}$$

$$s_3 = i\sqrt{\frac{K_{yy}}{M}}$$

$$s_4 = -i\sqrt{\frac{K_{yy}}{M}} \tag{44}$$

Referring to Equation 42 we see that our two natural frequencies are

$$v_1 = \sqrt{\frac{K_{xx}}{M}}$$

$$v_2 = \sqrt{\frac{K_{yy}}{M}} \tag{45}$$

which are the natural frequencies of two simple, uncoupled, spring-mass systems.

Bearing Response

When a rotor supported in a fluid film bearing is subjected to an arbitrary dynamic loading W′(t), linearized response motions x′(t) and y′(t) would require numerical integration of Equations 32 and 33. Frequently, however, dynamic loading is harmonic in nature and is most commonly due to shaft unbalance. Such a rotating dynamic loading can be described by the following equations:

$$W_x' = A\cos\omega t$$

$$W_y' = A\sin\omega t \tag{46}$$

where A is the amplitude of the loading and ω is the frequency. Substituting into Equations 32 and 33 we obtain

Copyright © 1983 CRC Press LLC

$$M\frac{d^2x'}{dt^2} + B_{xx}\frac{dx'}{dt} + B_{xy}\frac{dy'}{dt} + K_{xx}x' + K_{xy}y' = A\cos\omega t \quad (47)$$

$$M\frac{d^2y'}{dt^2} + B_{yx}\frac{dx'}{dt} + B_{yy}\frac{dy'}{dt} + K_{yx}x' + K_{yy}y' = A\sin\omega t \quad (48)$$

The following particular solution for x′ and y′ satisfies the right-hand sides of Equations 47 and 48:

$$x'(t) = A\alpha_x\cos\omega t - A\beta_x\sin\omega t \quad (49)$$

$$y'(t) = A\alpha_y\cos\omega t - A\beta_y\sin\omega t \quad (50)$$

where:

$$\alpha_x = \frac{\psi(K_{yy} - M\omega^2) + \phi\omega B_{yy} - \psi\omega B_{xy} + \phi K_{xy}}{\psi^2 + \phi^2}$$

$$\beta_x = \frac{\psi\omega B_{yy} - \phi(K_{yy} - M\omega^2) + \psi K_{xy} + \phi\omega B_{xy}}{\psi^2 + \phi^2}$$

$$\alpha_y = \frac{\psi\omega B_{xx} - \phi(K_{xx} - M\omega^2) - \psi K_{yx} - \phi\omega B_{yx}}{\psi^2 + \phi^2}$$

$$\beta_y = \frac{-\psi(K_{xx} - M\omega^2) - \phi\omega B_{xx} - \psi\omega B_{yx} + \phi K_{yx}}{\psi^2 + \phi^2}$$

$$\psi = \omega^4M^2 + \omega^2[-B_{xx}B_{yy} + B_{xy}B_{yx} - M(K_{xx} + K_{yy})] + K_{xx}K_{yy} - K_{xy}K_{yx}$$

$$\phi = -\omega^3M(B_{xx} + B_{yy}) + \omega(B_{xx}K_{yy} + B_{yy}K_{xx} - B_{xy}K_{yx} - B_{yx}K_{xy})$$

Equations 49 and 50 give the forced vibration response solution to Equations 47 and 48 as distinct from the natural frequency or free vibration solutions discussed earlier. Both forced and free vibration frequencies may be present in the total frequency spectrum of a vibrating rotor. Unless the natural frequency vibrations are excited by random forces, however, they will decay exponentially with time for a stable bearing. Forced vibrations, however, will be sustained at the stable amplitudes given by Equations 49 and 50.

For some insight into bearing response, consider a simplified bearing for which cross-coupling stiffness terms are zero and damping may be neglected. Equations 49 and 50 reduce to:

$$x'(*) = \frac{A}{(K_{xx} - M\omega^2)}\cos\omega t$$

$$y'(*) = \frac{A}{(K_{yy} - M\omega^2)}\sin\omega t \quad (51)$$

When the dynamic loading frequency ω becomes equal to one of the natural frequencies as given by Equation 45, the response amplitude becomes infinitely large in either the x or y direction.

For purpose of discussion, assume that $K_{yy} < K_{xx}$. For values of ω less than $(K_{yy}/M)^{1/2}$, i.e., below the critical speed, Equations 51 yield the response orbit shown schematically in Figure 11a. This ellipse is traced out by the center of the rotor whirling in the same direction as shaft rotation. In this region, the y amplitude will always be greater than the x.

Copyright © 1983 CRC Press LLC

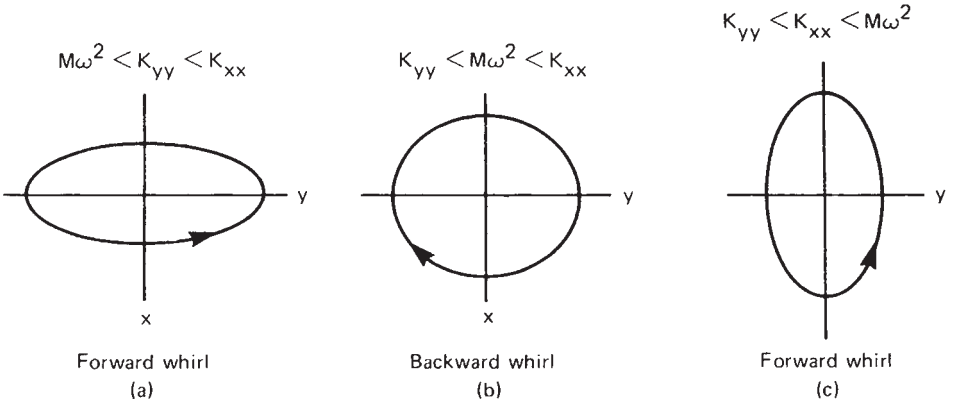

FIGURE 11. Typical response ellipses for undamped bearing with no cross-coupling coefficients.

For values of ω between v_1 and v_2, the response orbit will be backward whirling as shown in Figure 11b. As ω increases from v_1 to v_2, the y amplitude will decrease and the x amplitude will increase. For values of ω greater than v_2 in Figure 11c, the response orbit again reverts to forward whirl with the x amplitude greater. With damping and cross-coupling terms included, the axis of response ellipses will, in general, be inclined at an angle to the horizontal. Damping also limits response amplitude as the rotor passes through critical speeds.

Bearing Stability

As noted earlier, a bearing is unstable if the real part, λ, of any roots of characteristic Equation 41 are positive. A simpler criterion for stability is the "threshold of stability", i.e., the point where λ passes through zero going from negative to positive and the corresponding value for $s = \lambda + iv$ becomes purely imaginary.

Operating conditions for this threshold are determined by setting $s = iv$ and then solving Equation 41 to determine what critical values of shaft mass M_c and frequency v_c are required in order that the rotor-bearing system be at the threshold of stability.

$$v_c^2 = \frac{(K_{xx} - K)(K_{yy} - K) - K_{xy}K_{yx}}{B_{xx}B_{yy} - B_{xy}B_{yx}} \tag{52}$$

$$M_c = K/v_c^2 \tag{53}$$

where

$$K = \frac{K_{xx}B_{yy} + K_{yy}B_{xx} - K_{xy}B_{yx} - K_{yx}B_{xy}}{B_{xx} + B_{yy}} \tag{54}$$

v_c is the instability whirl frequency while M_c is the critical rotor mass for onset of instability. If the actual shaft mass is less than M_c, the system will be stable and conversely.

These stability formulas may be extended to a simple, symmetrical, flexible rotor of effective shaft stiffness K_R, supported on two equal bearings, by modifying the expression for M_c as follows:

$$M_c = \frac{1}{v_c^2} \quad \frac{2KK_R}{2K + K_R} \tag{55}$$

Greater shaft flexibility (lower K_R) tends to decrease M_c, i.e., decrease stability. Shaft

Copyright © 1983 CRC Press LLC

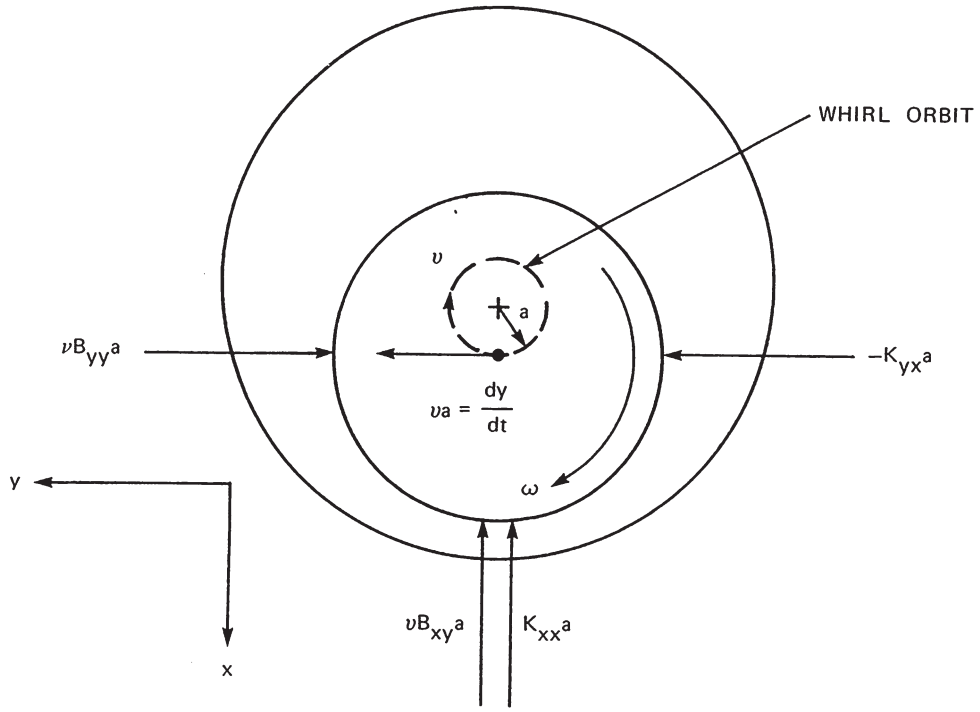

FIGURE 12. Dynamic forces acting on whirling journal.

stiffness, K_R, can be determined approximately by dividing the weight of the rotor by the mid-span deflection resulting from that weight.

Figure 12 indicates the role played by the various bearing coefficients in stability. The journal is shown whirling at the frequency v in a circular orbit of radius a about its equilibrium position. At the instant depicted, the journal center is displaced in the x direction while the velocity of the bearing center is in the y direction and given by dy/dt = va. If dynamic forces acting on the journal in both the x and y directions are assumed to be in equilibrium, the journal is just at the "threshold" of instability and the whirl orbit is neither growing or decaying. Then

$$-K_{yx}a = B_{yy}va \text{ (y direction)}$$

$$K_{xx}a + B_{xy}va = Mv^2 a \text{ (x direction)} \quad (56)$$

In the y direction, cross-coupling force $-K_{yx}a$ tending to drive the journal in whirl must be balanced by damping term $B_{yy}va$. In the x direction, restoring force, $K_{xx}a + B_{xy}va$, tending to increase the orbit, must balance centrifugal force Mv^2a which tends to increase the orbit. The first equation determines the whirl frequency

$$v = -K_{yx}/B_{yy} \quad (57)$$

Typically, for fixed arc bearings operating at light loads, v is very close to half the journal rotational speed. As loading increases, v decreases as the bearing becomes more stable.

The equation for the x direction gives the "critical" shaft mass M_c necessary for the system to be at the threshold of instability:

Copyright © 1983 CRC Press LLC

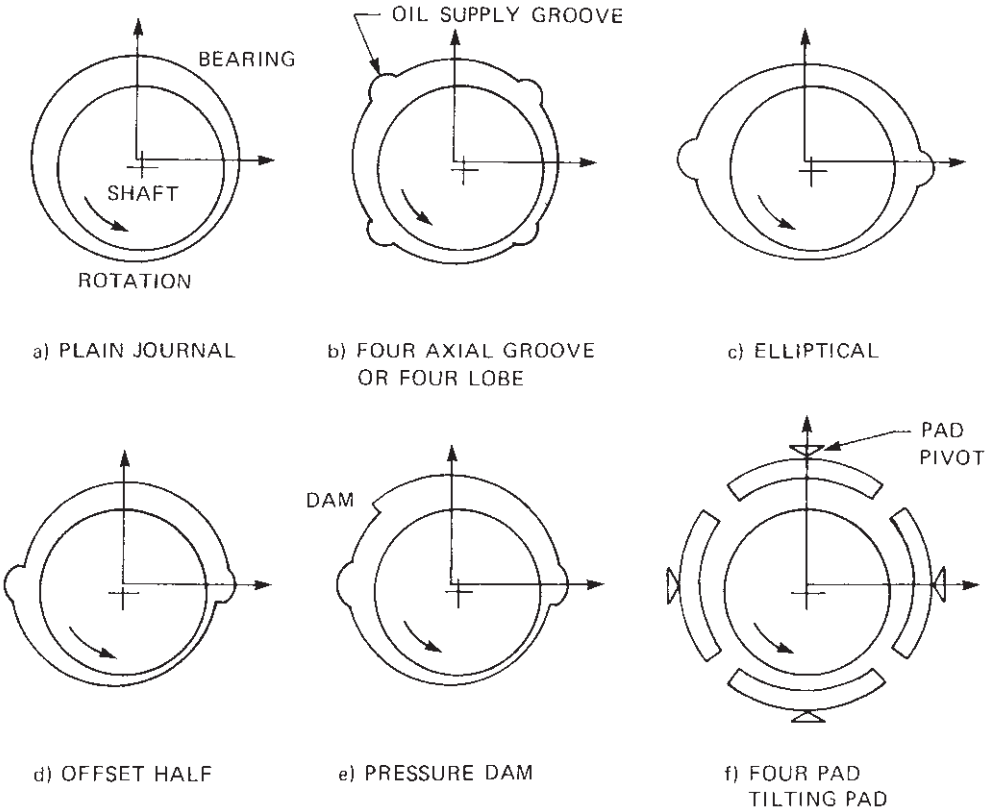

FIGURE 13. Geometry for various bearing types. (From Allaire, P. E., in *Fundamentals of the Design of Fluid Film Bearings,* Rhode, S. M., Maday, C. J., and Allaire, P. E., Eds., American Society of Mechanical Engineers, New York, 1979. With permission.)

$$M_c = (K_{xx} + B_{xy}\nu)/\nu^2 \tag{58}$$

where ν would be given by the preceding equation. If the actual shaft mass is less than M_c, the whirl orbit will diminish in amplitude (system is stable) while if the actual shaft mass is larger, the system will be unstable.

The above analytical exercise is not valid because it considers only one point on the orbit. In general, forces change as the shaft moves about the orbit and what happens "on average" determines system stability. The exercise does identify, however, the role of cross-coupling terms in promoting whirl, the type of balance which determines the whirl frequency ratio, and a critical mass criterion for stability.

Design of Bearings For Optimum Dynamic Performance

Preceding equations provide tools for evaluating bearing dynamic behavior from stiffness and damping coefficients. Fortunately, such data is being published for a variety of bearing geometries (References 22 to 25). Some bearing types in common use are shown schematically in Figure 13.[26] The first two bearings, the plain journal and the four-axial groove, are circular in shape. The arcs of elliptical and four-lobe bearings are displaced inwards some fraction of the bearing clearance to introduce preload. In bearing (d), the bearing arcs are displaced sideways for preload. Bearing (e) is usually circular but with a groove machined over a portion of one of the bearing arcs, the circumferential end of the groove being a dam.

Tilting pad bearing (f) is the most stable of all and is commonly employed in high-speed

Copyright © 1983 CRC Press LLC

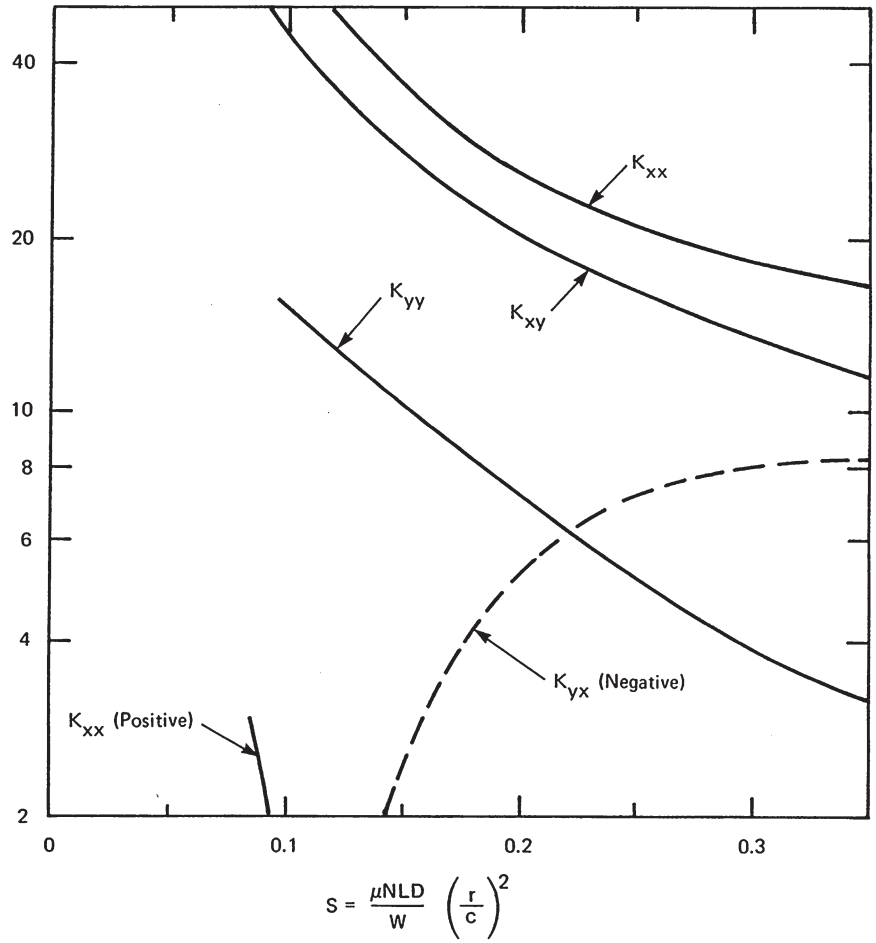

FIGURE 14. Elliptical bearing stiffness coefficients. L/D = 0.5; preload = 0.5. (From Allaire, P. E., Nicholas, J. C., Gunter, E. J., and Pan, C. H. T., Incompressible Fluid Film Bearings, U.S.A.F. Tech. Rep. AFAPL-TR-78-6, Air Force Aero Propulsion Laboratory, Wright-Patterson Air Force Base, Ohio, March 1980.)

machinery. Since each arc is free to pivot, the center of pressure generated in each bearing arc must be opposite the pivot point. Thus, if the shaft in Figure 13f moves directly down toward the bottom pad, the resultant force acts directly up, eliminating the cross-coupling force components which contribute to instability.

Stiffness and damping for fluid film bearings are usually presented in terms of a dimensionless stiffness coefficient Kc/W and a dimensionless damping coefficient ωBc/W plotted or tabulated as a function of either Sommerfeld Number $S = (\mu NLD/W)(r/c)^2$ or eccentricity ratio $\epsilon = e/c$. A typical plot of $\overline{K}$ vs. S for an elliptical bearing is shown in Figure 14.[22] As load increases in Figure 14, S decreases and the cross-coupling coefficient K_{yx} decreases to provide increased stability. A common cure for unstable bearing designs is to increase unit load W/LD by decreasing the bearing length.

Relative stability of some bearing types in Figure 15[26] is based on threshold of stability analysis represented by Equations 52 to 54. In this case, stability results are plotted in terms of a dimensionless critical mass $\overline{M}_c$ defined as $\omega\sqrt{cM_c/W}$. Figure 16 shows the corresponding whirl ratio v_c/ω at the threshold of instability.

Copyright © 1983 CRC Press LLC

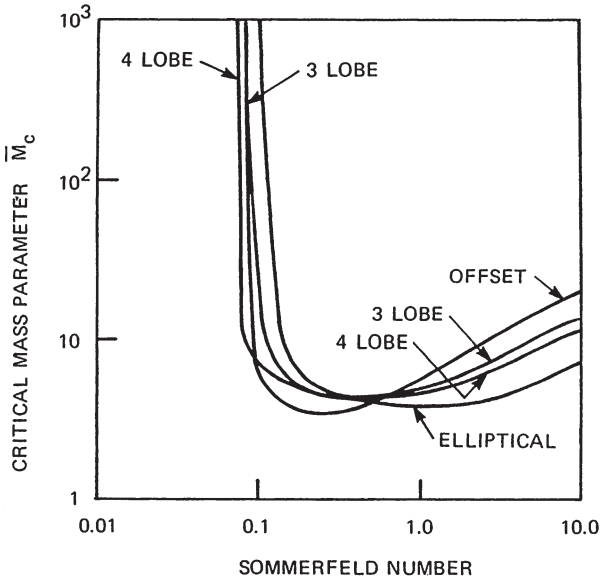

FIGURE 15. Linearized bearing stability for a rigid rotor (elliptical, 3-lobe and 4-lobe bearings have preload = 0.5). Offset bearing has 0.5 offset. (From Allaire, P. E., in *Fundamentals of the Design of Fluid Film Bearings,* Rohde, S. M., Maday, C. J., and Allaire, P. E., Eds., American Society of Mechanical Engineers, New York, 1979. With permission.)

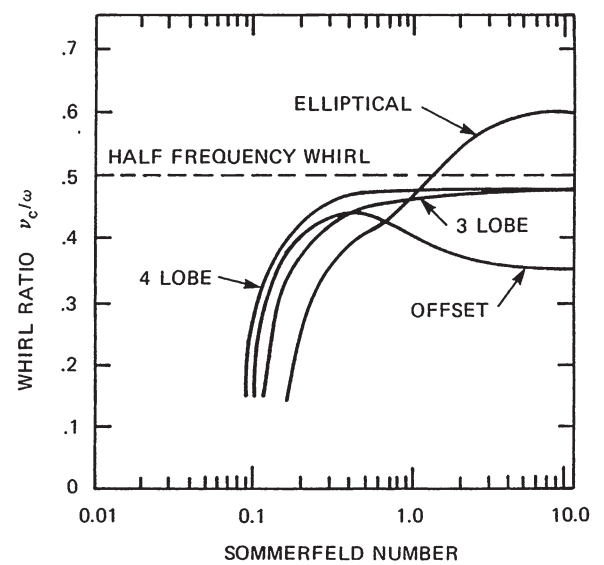

FIGURE 16. Whirl speed ratio vs. Sommerfeld number. (From Allaire, P. E., in *Fundamentals of the Design of Fluid Film Bearings,* Rohde, S. M., Maday, C. J., and Allaire, P. E., Eds., American Society of Mechanical Engineers, New York, 1979. With permission.)

Copyright © 1983 CRC Press LLC

NOMENCLATURE

B	= Bearing length
c	= Journal bearing radial clearance
D	= Journal diameter
e	= Eccentricity
F_f	= Friction force
h_o	= Slider minimum film thickness
h_1	= Slider maximum film thickness
h	= Film thickness
L	= Bearing width
N	= Rotational speed, cycles per second
P	= Pressure
Q	= Volumetric flow rate
q_x	= x-Component of lubricant flux
q_y	= y-Component of lubricant flux
r	= Radius, radial coordinate
R_e	= Reynolds number, cUp/μ
t	= Time
T	= Temperature
u	= x-Component of fluid velocity
U, U_1, U_2	= x-Components of surface velocities
U_r	= Radial component of surface velocity in cylindrical coordinates
v	= y-Component of fluid velocity
V, V_1,V_2	= y-Components of surface velocities
V	= Tangential component of velocity in cylindrical coordinates
w	= z-Component of fluid velocity
$\underline{W}$	= Load capacity
$\overline{X}$	= Center of pressure coordinates
$\in$	= Eccentricity ratio e/c
θ	= Journal bearing angular coordinate
μ	= Dynamic viscosity
ρ	= Density
δ	= Thrust bearing angular coordinate
ψ	= Journal bearing attitude angle
ω	= Angular velocity
v	= Kinematic viscosity μ/ρ, vibration frequency

REFERENCES

1. **Booker, J. F.,** A table of the journal-bearing integral, *Trans. ASME Ser. D,* 87, 533, 1965.
2. **Schlichting, H.,** *Boundary Layer Theory,* 6th ed., McGraw-Hill, New York, 1968.
3. **Taylor, G. I.,** Stability of a viscous liquid contained between two rotating cylinders, *Philos. Trans. R. Soc. London Ser. A,* 223, 289, 1923.
4. **Vohr, J. H.,** An experimental study of Taylor vortices and turbulence in flow between eccentric rotating cyclinders, *Trans. ASME Ser. F,* 90, 285, 1968.
5. **DiPrima, R. C. and Stuart, J. T.,** Non-local effects in the stability of flow between eccentric rotating cylinders, *J. Fluid Mech.,* 54, 393, 1972.
6. **Mobbs, F. R. and Younes, M. A.,** The Taylor vortex regime in the flow between eccentric rotating cylinders, *Trans. ASME Ser. F,* 96, 127, 1974.

Copyright © 1983 CRC Press LLC

7. **Frene, J. and Godet, M.,** Flow transition criteria in a journal bearing, *Trans. ASME Ser. F,* 96, 135, 1974.
8. **Gross, W. et al.,** *Fluid Film Lubrication,* John Wiley & Sons, New York, 1980.
9. **Taylor, G. I.,** Fluid friction between rotating cylinders. I. Torque measurements, *Proc. R. Soc. A.,* 157, 546, 1936.
10. **Constantinescu, V. N.,** On turbulent lubrication, *Proc. Inst. Mech. Eng.,* 173(38), 881, 1959.
11. **Elrod, H. G. and Ng, C. W.,** A theory for turbulent fluid films and its application to bearings, *J. Lubr. Technol., Trans. ASME Ser. F,* 89(3), 346, 1967.
12. **Hirs, G. G.,** A bulk theory for turbulence in lubricant films, *J. Lubr. Technol., Trans. ASME,* 95(2), 137, 1973.
13. **Ng, C. W. and Pan, C. H. T.,** A linearized turbulent lubrication theory, *J. Basic Eng., Trans. ASME,* 87(4), 675, 1965.
14. **Constantinescu, V. N.,** Basic relationships in turbulent lubrication and their extension to include thermal effects, *J. Lubr. Technol., Trans. ASME,* 95, 147, 1973.
15. **Constantinescu, V. N., Pan, C. H. T., and Hsing, F. C.,** A procedure for the analysis of bearings operating in the transition range between laminar and fully developed turbulent flow, *Rev. Roum, Sci. Techn.-Mech. Appl.,* 16(5), 945, 1971.
16. **Reddeclif, J. M. and Vohr, J. H.,** Hydrostatic bearings for cryogenic rocket engine turbopumps, *J. Lubr. Technol., Trans. ASME Ser. F,* 91(3), 557, 1969.
17. **Capitao, J. W., Gregory, R. S., and Whitford, R. P.,** Effects of high operating speeds on tilting pad thrust bearing performance, *Trans. ASME Ser. F,* 98, 73, 1976.
18. **Vohr, J. H.,** Prediction of the operating temperature of thrust bearings, *J. Lubr. Technol., Trans. ASME,* 103(1), 97, 1981.
19. **Roben, G. D.,** private communication, General Electric Company, 1981.
20. **Abramovitz, S.,** Turbulence in a tilting-pad thrust bearing, *Trans. ASME,* 78, 7, 1956.
21. **Gregory, R. S.,** Performance of thrust bearings at high operating speeds, *Trans. ASME Ser. F,* 96, 7, 1974.
22. **Allaire, P. E., Nicholas, J. C., Gunter, E. J., and Pan, C. H. T.,** Rotor Bearing Dynamics Technology Design Guide, V. Dynamic Analysis of Incompressible Fluid Film Bearings, U.S.A.F. Tech. Rep. AFAPL-TR-78-6, Air Force Aero Propulsion Laboratory Wright-Patterson Air Force Base, Ohio, March 1980.
23. **Nicholas, J. C., Gunter, E. J., and Allaire, P. E.,** Stiffness and damping coefficients for the five-pad tilting pad bearing, *ASLE Trans.,* 22(2), 113, 1979.
24. **Nicholas, J. C., Allaire, P. E., and Lewis, D. W.,** Stiffness and damping coefficients for finite length step journal bearings, *ASLE Trans.,* 23(4), 353, 1980.
25. **Lund, J. W. and Thomsen, K. K.,** A calculation method and data for the dynamic coefficients of oil-lubricated journal bearings, in *Topics in Fluid Film Bearing and Rotor Bearing System Design and Optimization,* American Society of Mechanical Engineers, New York, 1978, 1.
26. **Allaire, P. E.,** Design of journal bearings for high speed rotating machinery, in *Fundamentals of the Design of Fluid Film Bearings,* Rohde, S. M., Maday, C. J., and Allaire, P. E., Eds., American Society of Mechanical Engineers, New York, 1979.

Copyright © 1983 CRC Press LLC